Molecular Crystals and Liquid Crystals

Publication details, including instructions for authors and subscription information:
http://www.tandfonline.com/loi/gmcl20

Mesomorphism of Four-Coordinated Four-Chained Metal Complexes Based on Pyrazolylpyridine Derivatives

Paloma Ovejero [a], M. José Mayoral [a], Mercedes Cano [a], José A. Campo [a], José V. Heras [a], Paula Fernández-Tobar [a], Marta Valién [a], Elena Pinilla [a b] & M. Rosario Torres [b]

[a] Departamento de Química Inorgánica I, Facultad de Ciencias Químicas, Universidad Complutense, Madrid, Spain

[b] Laboratorio de Difracción de Rayos-X, Facultad de Ciencias Químicas, Universidad Complutense, Madrid, Spain

Version of record first published: 22 Sep 2010

To cite this article: Paloma Ovejero, M. José Mayoral, Mercedes Cano, José A. Campo, José V. Heras, Paula Fernández-Tobar, Marta Valién, Elena Pinilla & M. Rosario Torres (2008): Mesomorphism of Four-Coordinated Four-Chained Metal Complexes Based on Pyrazolylpyridine Derivatives, Molecular Crystals and Liquid Crystals, 481:1, 34-55

To link to this article: http://dx.doi.org/10.1080/15421400701834005

Mol. Cryst. Liq. Cryst., Vol. 481, pp. 34–55, 2008

ISSN: 1542-1406 print/1563-5287 online
DOI: 10.1080/15421400701834005

Taylor & Francis
Taylor & Francis Group

Mesomorphism of Four-Coordinated Four-Chained Metal Complexes Based on Pyrazolylpyridine Derivatives

Paloma Ovejero[1], M. José Mayoral[1], Mercedes Cano[1], José A. Campo[1], José V. Heras[1], Paula Fernández-Tobar[1], Marta Valién[1], Elena Pinilla[1,2], and M. Rosario Torres[2]
[1]Departamento de Química Inorgánica I, Facultad de Ciencias Químicas, Universidad Complutense, Madrid, Spain
[2]Laboratorio de Difracción de Rayos-X, Facultad de Ciencias Químicas, Universidad Complutense, Madrid, Spain

*A homologous series of four-chained silver(I) and zinc(II) metal complexes based on the coordination of two NN′-bidentate ligands $pz^{R2}py$ 2-[3,5-bis(4-alkyloxy)phenyl]-pyrazol-1-yl]pyridine ($R = C_6H_4OC_nH_{2n+1}$, $n = 16, 18$) have been synthesised. All compounds $[M(pz^{R2}py)_2][A]_m$ ($M = Ag$, $m = 1$, $n = 16, 18$, $A = PF_6^-$ (**1,2**), SbF_6^- (**3,4**), $CF_3SO_3^-$ (OTf^-) (**5,6**), NO_3^- (**7,8**); $M = Zn$, $m = 2$, $n = 16, 18$, $A = NO_3^-$ (**9,10**)) exhibit liquid crystal properties showing enantiotropic SmA phases, independently of the starting $pz^{R2}py$ ligands (non-mesomorphism for $n = 18$ or monotropic liquid crystal for $n = 16$), as well as the coordination geometry.*

*The silver(I) derivatives $[Ag(pz^{R2}py)_2]^+$ containing PF_6^- and SbF_6^- as counteranions (**1–4**) are four-coordinated cationic complexes, but those containing OTf^- and NO_3^- (**5–8**) exhibit a five-coordinated metal environment with distorted base-square pyramidal/trigonal bipyramidal geometry involving the counteranion. For the zinc(II) related compounds $[Zn(pz^{R2}py)_2][NO_3]_2$ (**9–10**), the tetrahedral metal environment is also distorted by the presence of coordinative interactions with the NO_3^- groups.*

*Neutral tetrahedral compounds $[ZnCl_2(pz^{R2}py)]$ ($R = C_6H_4OC_nH_{2n+1}$, $n = 16$ (**11**), 18 (**12**), 1 (**13**)) have also been investigated. Crystal structure of the first member of this series with $n = 1$, $[ZnCl_2(pz^{An2}py)]$ (**13**), has been characterised by single crystal X-ray diffraction. The molecules adopt the tetrahedral coordination environment with a planar ZnNNCN core. That structure for the related compounds containing longer alkyloxy chains (**11–12**) suggests a rod-like molecular shape in agreement with their observed liquid crystal lamellar phases.*

Financial support from the DGI of the Ministerio de Educación y Ciencia (Project No. CTQ2006-13344) and Universidad Complutense/Comunidad Autónoma de Madrid (UCM2006-910300) is gratefully acknowledged.

Address correspondence to Mercedes Cano, Departmento de Química Inorgánica I, Facultad de Ciencias Químicas, Universidad Complutense, Madrid, 28040, Spain. E-mail: mmcano@quim.ucm.es

Keywords: four-chained complexes; four-coordinated silver and zinc complexes; pyrazolylpyridine ligands; smectic mesophases; XRD studies

INTRODUCTION

We have previously reported the synthesis of *N*,*N*′-donor 2-[3,5-bis(4-alkyloxyphenyl)pyrazol-1-yl]pyridine ligands $pz^{R2}py$ ($R = C_6H_4OC_nH_{2n+1}$) and the liquid crystal properties of those containing chains with $n = 14$ and 16 carbon atoms, larger chains ($n = 18$) avoiding the mesomorphism [1]. Preliminary studies on the coordination chemistry on the first generation of linked $pz^{R2}py$ ligands with $PdCl_2$ or $[Pd(\eta^3-C_3H_5)]^+$ fragments led to tetracoordinated square-planar complexes showing smectic mesophases [1,2].

Now we are interested in determining the liquid crystalline impact of new ionic complexes not only by changing the metal centre but also the coordination environment geometry and by modifying the counteranions.

We firstly want to establish whether longer chain derivatives of *N*,*N*′-bidentate ligands $pz^{R2}py$ would produce liquid crystal ionic silver-tetracoordinated four-chained complexes of the type $[Ag(pz^{R2}py)_2][A]$ (A = counteranion) or five-coordinated $[Ag(pz^{R2}py)_2(A)]$ if the counteranion A is involved.

Related cationic *bis*-chelating complexes from disubstituted bipyridines $[Ag(L^n)_2][OTf]$ (L^n = 2,2′-bipyridine-4,4′-diamides; $OTf^- = CF_3SO_3^-$) have been described to have columnar mesomorphism [3], their tetrahedral geometry being proposed on the basis of the crystal structure of the non-substituted 2,2′-bipyridine silver complexes with anions such as BF_4^- and PF_6^- [4,5]. However, in a previous work we have described the X-ray crystal structure of the complex $[Ag(pz^{bp2}py)_2][OT]$ ($pz^{bp2}py$ = 2-[3,5-bis(4-butoxyphenyl)pyrazol-1-yl]pyridine) in which the silver atom is five-coordinated to the four nitrogen atoms of the two pyrazolylpyridine ligands and to an oxygen atom of the OTf^- anion [6] (Fig. 1a). In this way, the distorted square-base pyramidal/trigonal bipyramidal geometry around the metal gave rise to almost parallel pyrazole rings from the $pz^{bp2}py$ ligands and consequently the four-chains of the substituents describing a particular 'H' shape (Fig. lb). On this basis, we think that new related complexes of the type $[Ag(pz^{R2}py)_2][A]$ bearing longer chains on the pyrazole rings should be appropriate candidates to exhibit smectic mesomorphism (Fig. 1c).

More importantly we are interested in trying to elucidate what factors are responsible for either promoting or inhibiting the

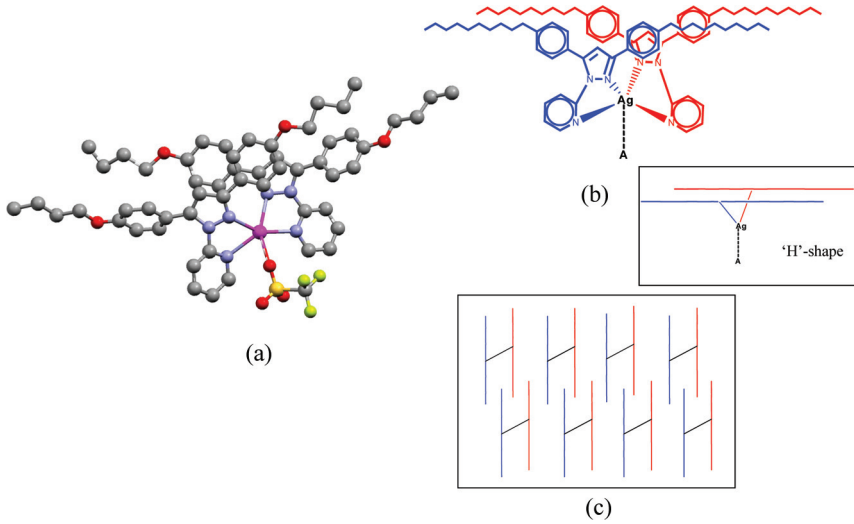

FIGURE 1 (a) Molecular structure of $[Ag(pz^{bp2}py)_2][OTf]$ [6]. (b) Schematic representation of the structure of $[Ag(pz^{bp2}py)_2][OTf]$ showing the 'H' shape, (c) Schematic representation of the potential packing of compounds with longer chains.

mesomorphism on tetrahedral complexes, this geometry being found to be the main impediment to have liquid crystal properties [7]. For this purpose and taking into account that in most of the tetracoordinated zinc derivatives containing *N*-donor ligands the metal atom adopts a tetrahedral geometry [8], we propose the study of new tetra-coordinated four-chained zinc compounds based on the *N*,*N*′-bidentate $pz^{R2}py$ ligands of the type $[Zn(pz^{R2}py)_2]^{2+}$.

In this context, it is also interesting to consider the previous results reported by Serrano *et al.* for the tetrahedral complexes $[ZnCl_2(Hpz^*)_2]$ ($Hpz^* = 3,5$-bis(4-decyloxyphenyl)pyrazole) and $[ZnCl_2(L_2m)]$ ($L_2m =$ bis[3,5-bis(4-decyloxyphenyl)pyrazol-1-yl]methane), which did not exhibit liquid crystal properties [9]. The absence of mesomorphism was attributed to the tetrahedral geometry which was responsible for the unfavourable angle between the mesogens, and in particular for the latter compound it was also attributed to the non-planar central metallacycle.

Following those precedents we think that, by using the bidentate ability of $pz^{R2}py$ ligands towards Zn^{2+} or $ZnCl_2$, a planar ZnNNCN metallacycle will be found, so favouring the organisation of the molecules in the mesophases. To prove this proposal, the crystal structure

of $[ZnCl_2(pz^{An2}py)]$ ($pz^{An2}py$ = 2-[3,5-bis(4-methoxyphenyl)pyrazol-1-yl]pyridine) was solved and used as a model for related compounds containing long-chained $pz^{R2}py$ ligands.

In this article we report the preparation and the liquid crystal properties of ionic four-coordinated four-chained complexes of the type $[M(pz^{R2}py)_2]^{m+}$ (M = Ag, m = 1; M = Zn, m = 2; R = $C_6H_4OC_nH_{2n+1}$, n = 16, 18; **1–10**) (Scheme 1a). The closely related neutral zinc derivatives $[ZnCl_2(pz^{R2}py)]$ (R = $C_6H_4OC_nH_{2n+1}$, n = 16, 18; **11–12**) have been also prepared and their liquid crystal behaviour described (Scheme lb). The X-ray crystal structure of $[ZnCl_2(pz^{An2}py)]$ (**13**) as a representative example is also reported.

RESULTS AND DISCUSSION

Synthetic and Characterisation Results

The $pz^{R2}py$ ligands were synthesised according to the methods previously described [1,2]. The silver complexes of general formula $[Ag(pz^{R2}py)_2][A]$ (R = $C_6H_4OC_nH_{2n+1}$ n = 16, 18; A = PF_6^- SbF_6^- $CF_3SO_3^-$ (OTf^-), NO_3^-; **1–8**) have been prepared by the reaction of $pz^{R2}py$ ligands with the corresponding silver salt AgA in a 1:2 (metal: ligand) stoichiometry. The reactions were carried out in THF as solvent and in the darkness during 24 h (Scheme 1a).

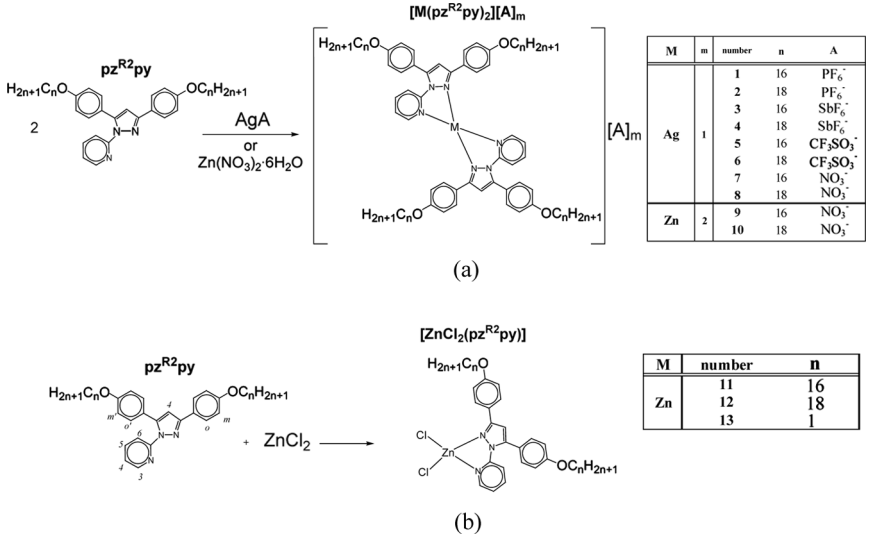

SCHEME 1 Synthesis of complexes **1–13** and nomenclature used in the work.

The related zinc derivatives $[Zn(pz^{R2}py)_2][NO_3]_2$ ($R = C_6H_4OC_nH_{2n+1}$, $n = 16$, 18; **9–10**) were prepared by a similar procedure using one equivalent of $Zn(NO_3)_2$ and two equivalents of the corresponding $pz^{R2}py$ ligand (Scheme 1a).

The neutral complexes $[ZnCl_2(pz^{R2}py)]$ ($R = C_6H_4OC_nH_{2n+1}$, $n = 16$, 18, 1; **11–13**) were synthesised by the reaction of anhydrous $ZnCl_2$ and $pz^{R2}py$ in a stoichiometric amount in THF solution (Scheme 1b).

All the complexes were characterised by analytical and spectroscopical (IR and ^{1}H-NMR) techniques (see *Experimental Section)*. The results agree with the proposed formulations.

The IR spectra of **1–13** in the solid state show the characteristic bands of the $pz^{R2}py$ ligands scarcely modified upon coordination, as it has also been found in other pyrazolypyridine derivatives [1,2,10,11]. In addition, bands of the corresponding counteranions in **1–10** are also observed (Table 1). By comparing the values of the absorption bands of the anionic groups with those observed in metal salts [12,13], we can suggest an ionic nature of the counteranions in the complexes, although the presence of metal-anion interactions cannot be excluded specially in those containing OTf^- or NO_3^-.

TABLE 1 Characteristic IR Bands of the Counteranions for the Complexes **1–10**

	ν_{as}(PF)	δ(FPF)
PF_6^- [a]	**840**	**559**
1	842	558
2	841	556
	ν_{as}(SbF)	
SbF_6^- [a]	**669**	
3	660	
4	659	
	$\nu_{as}(SO_3)$	$\nu_s(SO_3)$
$AgCF_3SO_3$ [b]	**1270**	**1043**
5	1274	1029
6	1278	1028
	Vd(NO)	δ(ONO)
$NaNO_3$ [a]	**1405**	**831**
7	1384	828
8	1385	825
9	1385	840
10	1384	839

[a]Ref. [12]
[b]Refs. [13,14]

For instance, the two peaks at *ca*. 1275 and 1030 cm^{-1} observed in **5** and **6** from the OTf^- groups (Table 1) are close but lower than those observed in AgOTf which presents the silver atom coordinated to the anion [13,14]. In addition, the previously reported complexes $[Ag_2L^3(OTf)_2(CH_3COCH_3)]_\infty$, $[Ag_2L^3(OTf)_2]_\infty$ and $[Ag_2L^2(OTf)_2]$ (L^3 = l,3-bis(phenylthio)propane; L^2 = dibenzo[*b,def*]chrysene) exhibited those bands at *ca*. 1260 and 1035 cm^{-1} in agreement with the presence of a OTf^- group coordinated to the silver atom [13,15]. Taking into account these results, as well as the structural analysis of the similar complex $[Ag(pz^{bp2}py)_2][OTf]$ which exhibited a five-coordinated metal environment produced by coordination of two $pz^{bp2}py$ ligands and the OTf^- anion (Fig. 1a) and a $\nu(SO_3)$ frequency of the latter at 1273 cm^{-1} [6], we can propose a related five-coordinated environment around the silver(I) in **5** and **6**.

On the other hand, the bands from the NO_3^- group in **7-10** at *ca*. 1385 and 830 cm^{-1} (Table 1) appear at the same frequencies than those observed in $[Ag(Hpz^{NO2})_2][NO_3]$ (Hpz^{NO2} = 3,5-dimethyl-4-nitropyrazole) containing coordinative interactions Ag $\cdots$ $O(NO_3)$ [16]. This feature suggests potential similar interactions in our complexes.

At difference of the strongly coordinating counteranions OTf^- and NO_3^-, groups such as PF_6^- or SbF_6^- present a weak coordinative ability and they maintain their ionic nature in the complexes **1–4** herein studied. This is supported by the corresponding bands at *ca*. 840 and 555 cm^{-1} (PF_6^-) and *ca*. 660 cm^{-1} (SbF_6^-) observed in the IR spectra of **1,2** and **3,4**, respectively. These values compare well with those reported for ionic compounds containing PF_6^- or SbF_6^- as counteranions [13,17–20].

The ′H-NMR spectra of all silver and zinc derivatives **1–10** exhibit the $pz^{R2}py$ signals corresponding with the equivalence of both ligands as well as the unequivalence of the substituents at the pyrazole groups (see *Experimental Section)*. The latter feature was also observed for the neutral $[ZnCl_2(pz^{R2}py)]$ complexes **11–13** (see *Experimental Section)*. In particular two signals for the OCH_2 group from the $C_6H_4OC_nH_{2n+1}$ substituents appear at *ca*. 4 ppm, their separation varying with the nature of the counteranion A.

Crystal Structure of $[ZnCl_2(pz^{An2}py)]$

Different attempts to grow adequate crystals of the compounds described in this work were unsuccessful. Therefore, we tried to obtain crystals of compounds bearing shorter chains at the periphery which could be used as a model to explain the behaviour of the mesophases.

On these basis, we have prepared the complex [$ZnCl_2$(pz^{An2}py)] (**13**) as a representative member of the homologues studied. The crystal structure and the crystal packing of this compound are given in Figure 2. Selected bond distances and angles are listed in the legend of Figure 2.

The environment around the zinc atom is defined by two nitrogen atoms of the pz^{An2}py ligand and two chorides, giving rise to a distorted

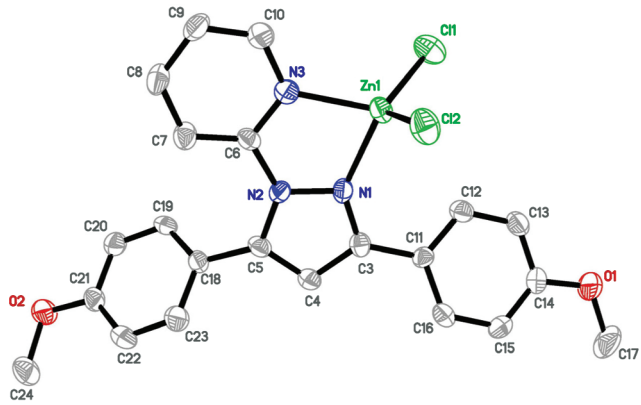

(a)

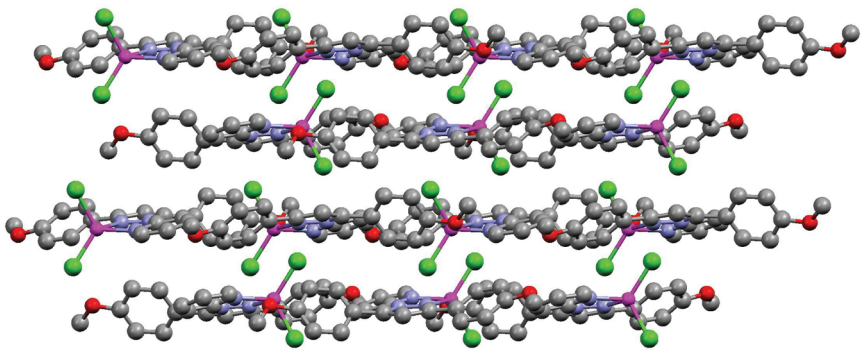

(b)

FIGURE 2 (a) ORTEP plot of **13** with 40% probability. Hydrogen atoms have been omitted for clarity. Selected bond distances (Å) and angles (°): Zn1–Cl1 2.184(1), Zn1–C12 2.206(1), Zn1–N1 2.047(3), Zn1–N3 2.058(3), N1–Zn1–N3 77.4(1), N1–Zn1–Cl1 123.0(1), N3–Zn1–Cl1 113.6(1), N1–Zn1–C12 108.0(1), N3–Zn1–Cl2 111.7(1), Cl1–Zn1–Cl2 116.8(1). b) Crystal packing of 13 showing the layer-like characteristics.

tetrahedral geometry as deduced by the dihedral angle formed between the Zn1N1N3 and Zn1Cl1C12 planes of 84.8(1)°. The major deviation from the ideal is imposed by the bite angle N1–Zn1–N3 of the bidentate $pz^{An2}py$ ligand. The Zn1–N1 and Zn1–N3 bonds form the basis of a five-membered metallocycle Zn1N1N2C6N3, where the C6 atom deviates −0.081(4) Å. The Zn–N and Zn–Cl distances compare well with other examples of the literature [9,21–27].

The pyrazole and pyridine planes are almost coplanar respect to each other and form a dihedral angle of 8.4(2)°. The benzene planes of the substituents are twisted with respect to the own pyrazole plane with dihedral angles of 50.2(2) and 28.0(1)°. The largest angle corresponds, as expected, to the benzene plane closer to the pyridine ring. In this disposition, the benzene planes are twisted respect to each other at an angle of 45.5(2)°.

The molecules are in layers in an antiparallel fashion with the chloride ligands disposes in *pseudo-axial* positions related to the main molecular plane defined by the pyrazole and pyridine groups.

To a supramolecular level, weak C···O hydrogen-bond interactions between different molecules (C10···O2(x, $\frac{1}{2}-y$, $\frac{1}{2}+z$): 3.38(1) Å; C10–H10···O2 angle 141.7°) define chains which are propagated along the c axis. Then, the structure can be considered as the layer-like type (Fig. 2b) but generating a 1D network.

By considering a similar environment for related compounds having long-chained $pz^{R2}py$ ligands, we suggest that the molecules exhibiting a rod-like shape will be arranged in a layer-like ordering as that of the SmA mesophases.

Thermal Studies

All complexes **1–12** exhibit liquid crystal properties. The phase transition temperatures from the first heating-cooling cycle of the DSC thermograms are given in Table 2.

The DSC thermograms of the silver and zinc derivatives **1–10** exhibit a similar pattern. We will take that of the compound $[Ag(pz^{R2}py)_2][SbF_6]$ ($R = C_6H_4OC_{16}H_{33}$; **3**) as a representative example (Fig. 3). The first heating shows endothermic transitions at 107°C ($\Delta H = 132.6\,kJmol^{-1}$) and 117°C ($\Delta H = 5.9\,kJmol^{-1}$), the first one corresponding with the transition of the crystal phase to the mesophase. The second peak having a relatively small enthalpy corresponds to the transition from the mesophase to the isotropic liquid. On cooling only one exothermic peak at 116°C ($\Delta H = -6.6\,kJmol^{-1}$) is registered and it corresponds to the formation of the mesophase, as it is observed by light-polarised optical microscopy (POM). The

TABLE 2 Thermal Data by DSC for the New Complexes **1–12**

	n = 16			n = 18		
A	Transition	T/°C	ΔH/kJmol^{-1}	Transition	T/°C	ΔH/kJmol^{-1}
[Ag(pz^{R2}py)$_2$][A]**(l–8)**						
		1			2	
PF_6^-	Cr → Cr′	92	65.7	Cr → Cr′	63	57
	Cr′ → Cr″	98	32.1	Cr′ → SmA	90	103.2
	Cr″ → SmA	114	7.8	SmA → IL	113	4.26
	SmA → 1L	127	6.5			
	IL → SmA	125	−2.9	IL → SmA	108	−1.8
	SmA → (a)	50*		SmA → (a)	50*	
		3			4	
SbF_6^-	Cr → SmA	107	132.6	Cr → SmA	107	127.1
	SmA → IL	117	5.9	SmA → IL	116	5.9
	IL → SmA	116	−6.6	IL → SmA	115	−5.2
	SmA → (a)	30*		SmA → (a)	54*	
		5			6	
$CF_3SO_3^-$	Cr → SmA	103	109.9	Cr → Cr′	73	29.3
	SmA → IL	112	6.1	Cr′ → SmA	96	58.1
				SmA → IL	118	6.6
	IL → SmA	112	−6.6	IL → SmA	85	−9.3
	SmA → (a)	55*		SmA → Cr	56	−66.1
		7			8	
NO_3^-	Cr → SmA	96	4.7	Cr → SmA	127	85.9
	SmA → IL	115	10.1	SmA → IL	133	4.55
	IL → SmA	103	−2.9	IL → SmA	133	−18.8
	SmA → (a)	40*		SmA → (a)	40*	
[Zn(pz^{R2}py)$_2$][A]$_2$**(9–10)**						
		9			10	
NO_3^-	Cr → SmA	78	188.4	Cr → SmA	66	80.2
	Sm_A → IL	89	6.31	SmA → IL	107	1
	IL → SmA	96	−2.6	IL → SmA	104	−3.1
	SmA → (a)	30*		SmA → (a)	51*	
[$ZnCI_2$(pz^{R2}py)] **(11–12)**						
		11			12	
	Cr → Cr′	64	7.1	Cr → SmA	88	
	Cr′ → SmA	92	50.3	SmA → IL	115	2.1
	SmA → IL	119	1.2			
	IL → SmA	117	−0.4	IL → SmA	114	−2.5
	SmA → (a)	60*		SmA → (a)	64*	

*Temperature observed by POM.

(a) At this temperature the texture of the SmA mesophase is maintained but no mobility is observed.

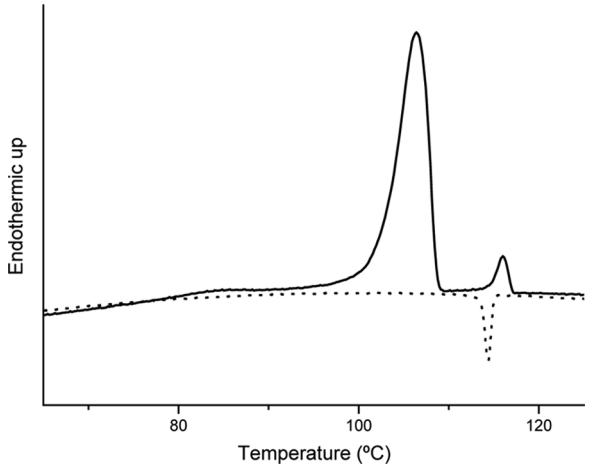

FIGURE 3 DSC trace of **3** in the 50–120°C range: first heating (straight line) and first cooling (dotted line).

mesophase was examined by optical observations showing the typical "fan-shaped" texture with homeotropic domains characteristic of a SmA mesophase (Fig. 4). Lowering the temperature until *ca*. 50°C (minimal temperature registered by the equipment), no more peaks are detected by DSC. However, optically it was possible to observe that at *ca*. 30°C, when the sample is subjected to a mecanical stress, the mobility of the phase disappears although the optical texture is maintained.

In general terms, for the other members of this family of compounds (**1–10**) a similar thermal behavior can be established. Some differences observed in **1**, **2** and **6** proceed from the presence of additional peaks in the first heating which are related with solid-to-solid phase transitions. It is also remarkable that for the silver complex $[Ag(pz^{R2}py)_2][OTf]$ ($R = C_6H_4OC_{18}H_{37}$; **6**) the mesophase-to-solid transition (SmA – Cr) could be observed. This result can be cautiously explained on the basis of a potential participation of the coordinative interactions from the triflate anion in the formation of the solid phase.

In the $[Ag(pz^{R2}py)_2][A]$ compounds **1–8**, the evident variation of the melting and clearing temperatures with the counteranion has two different trends. For those with 16 carbon atoms in the chains, there is a general increase in the melting and clearing temperatures in the order $NO_3^- < OTf < SbF_6^- < PF_6^-$. Upon increasing the chain length from 16 to 18 carbon atoms, the general tendency of both temperatures is inverse.

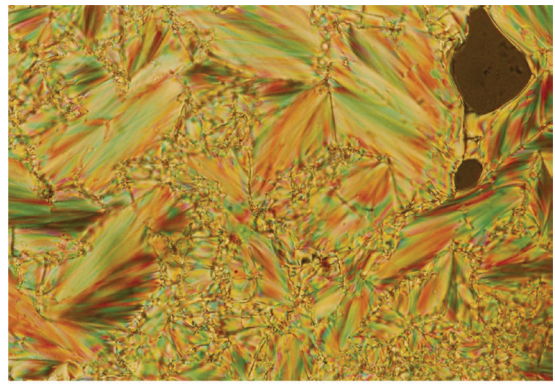

(a)

(b)

FIGURE 4 Textures of the SmA mesophases observed for (a) **1** on heating at 121°C and (b) **6** on cooling at 85°C.

On the other hand the phase transition temperatures of zinc derivatives $[Zn(pz^{R2}py)_2][NO_3]_2$ (**9–10**) are compared with those of the corresponding neutral complexes $[ZnCl_2(pz^{R2}py)_2]$ (**11–12**) with the same alkyloxy chain lengths, the former ones showing lower melting and clearing temperatures than the latter ones.

From the thermal results of all systems studied in this work, it can be established that the zinc derivatives $[Zn(pz^{R2}py)_2][NO_3]_2$ present the lower phase-transition temperatures, the complex **10** with 18 carbon atoms having the wider temperature range of the mesophase.

Structural Characterization of the Liquid Crystal Phase

The mesomorphic structures of these complexes were further studied by X-ray diffraction (Table 3). The silver series in the mesophase exhibit three sharp peaks (one strong followed by two weaker peaks) in the small-angle region and a diffuse halo scattering at 2θ of *ca*. 20°.

Figure 5 shows the XRD diffractogram of $[Ag(pz^{R2}py)_2][PF_6]$ ($R = C_6H_4OC_{16}H_{33}$; **1**) as a representative example. The small angle peaks measured at 115°C are assigned to (001), (002) and (003) reflections and indicate a well defined lamellar structure corresponding with a layer distance of 36.6 Å. The middle-angle halo indicates the fluid-like behaviour of the alkyloxy chains with an average domain of 4.4 Å. This diffraction pattern, together with the fan-shaped texture and homeotropic behaviour from POM, suggests the formation of SmA mesophases.

The other homologous complexes show similar XRD results exhibiting layer spacing of 36–38 Å in the mesophase (Table 3).

For the compounds of the type $[Ag(pz^{R2}py)_2][A]$, a molecular length L of the cationic part of *ca*. 41 Å or 45 Å (for chains of 16 and 18 carbon atoms, respectively) in a fully extended configuration was estimated from the X-ray crystalline structure of $[Ag(pz^{bp2}py)_2][OTf]$ [6]. Because the d-spacing of the smectic layers (36–38 Å) is slightly shorter than L (*ca*. 41–45 Å), we can deduce that the molecules are arranged in single molecules interdigitated layers.

The diffractograms at 30°C after cooling show in the small-angle region a strong peak followed by two weak peaks (not always observed), which are assigned to (001), (002) and (003) reflections and suggest a lamellar structure with a d-spacing varying from 40 to 42 Å (Table 3). In the middle-angle region, in addition to the broad diffuse scattering halo observed in the mesophase at 2θ of *ca*. 20° (d-spacing of *ca*. 4.5 Å (Fig. 6a), a new less intense but diffuse halo peak at the intermediate angles of *ca*. 12–14° (d-spacing of *ca*. 6.7–7.2 Å) is observed (Fig. 6b). The first one is related with the fluid-like behavior of the alkyloxy chains, but the presence of a distinct peak at *ca*. 6.7–7.2 Å can be indicative of a relatively ordered mesophase consistent with the observations by POM.

However, a similar X-ray pattern to that of the phase at 30°C has been recently reported for the liquid crystal phase of some Ni(II)-salen tetracoordinated complexes [28]. Those exhibited four reflections in the small-angles region corresponding to a lamellar phase, a diffuse band around 20° from the molten alkoxy chains and an additional peak at *ca*. 14° consistent with the stacking distance in a columnar structure in addition to the lamellar structure. Thus, these mesophases were assigned to a lamello-columnar phases (ColL) [28].

TABLE 3 Variable-temperature[a] XRD Diffraction Data for Complexes **1, 4, 5, 7, 10** and **12**

Complex	T/°C	Position/2θ	d-spacing/Å	Miller indices (hkl)
1	115*	2.4	36.6	(001)
		4.8	18.4	(002)
		7.2	12.2	(003)
		20.2	4.4	[b]
	30	2.1	41.3	(001)
		4.2	20.9	(002)
		6.4	13.9	(003)
		12.4	7.1	[c]
		20.8	4.3	[b]
4	110*	2.3	37.8	(001)
		19.0	4.6	[b]
	30	2.1	42.0	(001)
		13.1	6.7	[c]
		21.1	4.2	[b]
5	100*	2.4	36.3	(001)
		4.8	18.4	(002)
		20.5	4.3	[b]
7	90*	2.4	37.2	(001)
		4.6	19.3	(002)
		6.9	12.9	(003)
		19.9	4.5	[b]
	30	2.2	39.9	(001)
		12.4	7.2	[c]
		20.7	4.3	[b]
10	85	2.3	38.2	(001)
		4.5	19.8	(002)
		6.7	13.2	(003)
		19.5	4.5	[b]
	30	2.2	39.7	(001)
		4.4	20.0	(002)
		7.2	12.4	(003)
		12.5	7.1	[c]
		21.4	4.2	[b]
12	100*	2.3	37.7	(001)
		4.5	19.5	(002)
		6.8	13.0	(003)
		19.7	4.5	[b]
	30	2.2	40.5	(001)
		4.2	20.8	(002)
		12.5	7.1	[c]
		21.1	4.2	[b]

[a]Temperatures on cooling.
[b]Halo of the molten alkyloxy chains.
[c]See discussion.
*Temperature after mesophase is observed.

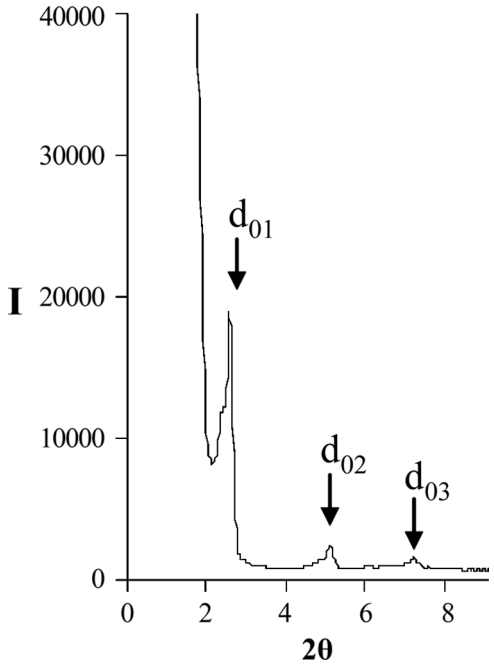

FIGURE 5 X-Ray diffraction pattern in the small-angles region of complex **1** at 115°C.

On this basis we could also propose a ColL mesophase for those observed at 30°C in our compounds, with stacking distances of *ca*. 6.7–7.2 Å in the *a*-axis direction and a lamellar distance of 40–42 Å. The ColL mesophase has an unusual columnar phase with the one-dimensional ordering of molecules within the smectic layers and there are few reports on metallomesogens with this kind of mesophase [28–36].

EXPERIMENTAL SECTION

Materials and Physical Measurements

All commercial reagents were used as supplied. The ligands 2-[3,5-bis(4-alkyloxy)phenyl]pyrazol-1-yl]pyridine $pz^{R2}py$ ($R = C_6H_4OC_nH_{2n+1}$; $n = 16, 18$) were prepared by procedures described in a previous work [1], Commercial solvents were dried prior to use.

Elemental analyses for carbon, hydrogen and nitrogen were carried out by the Microanalytical Service of Complutense University. IR

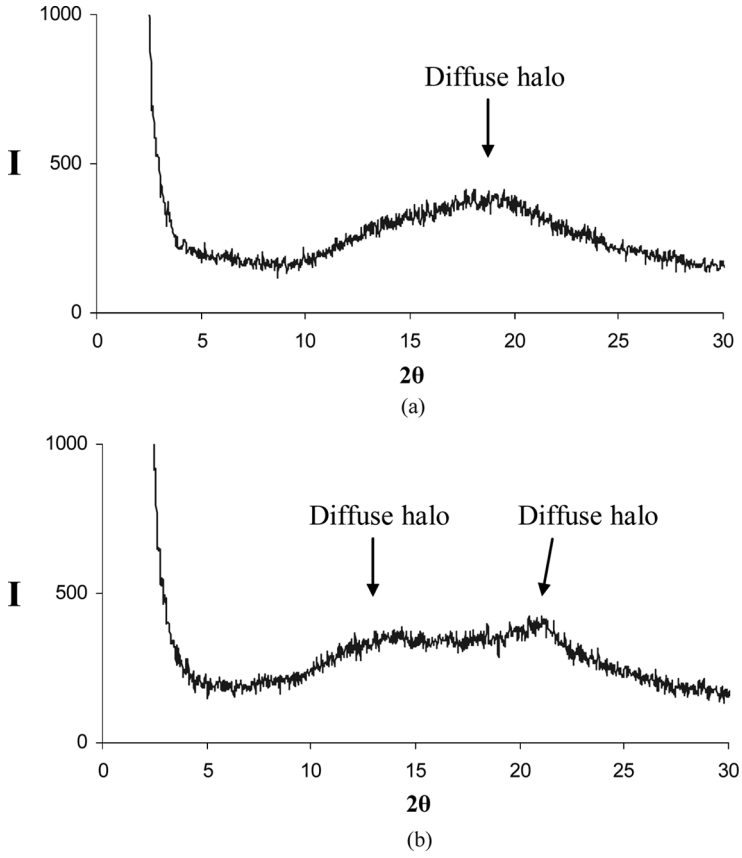

FIGURE 6 X-ray diffraction pattern in the middle-angles region of complex **4** (a) at 100°C and (b) at 30°C.

spectra were recorded on a FIT ThermoNicolet 200 spectrophotometer with samples as KBr pellets in the 4000–400 cm^{-1} region: vs (very strong), s (strong), m (medium), w (weak).

^1H NMR spectra were performed on a Bruker AC200 (200.13 MHz) of the NMR Service of Complutense University from solutions in $CDCI_3$. Chemical shifts δ are listed relative to TMS using the signal of the deuterated solvent as reference (7.26 ppm), and coupling constants J are in hertz. Multiplicities are indicated as s (singlet), d (doublet), t (triplet), m (multiplet), br (broad signal). The ^1H chemical shifts and coupling constants are accurate to ± 0.01 ppm and ± 0.3 Hz, respectively.

Phase studies were carried out by optical microscopy using an Olympus BX50 microscope equipped with a Linkam THMS 600 heating stage. The temperatures were assigned on the basis of optic observations with polarised light.

Measurements of the transition temperatures were made using a Perkin Elmer Pyris 1 differential scanning calorimeter with the sample (1–4 mg) sealed hermetically in aluminium pans and with a heating or cooling rate of 5–10°C min^{-1}.

The X-ray diffractograms at variable temperature were recorded on a Panalytical X'Pert PRO MPD diffractometer in a θ–θ configuration equipped with a Anton Paar HTK1200 heating stage (X-Ray Diffraction Service of Complutense University).

Preparation of the Complexes [Ag($pz^{R2}py)_2$][A] *($R = C_6H_4OC_nH_{2n+1}$; $n = 16, 18$; $A = PF_6^-$ (1,2), SbF_6^- (3,4), $CF_3SO_3^-$ (5,6), NO_3^- (7,8))*

To a solution of the corresponding 2-[3,5-bis(4-alkyloxy)phenyl]pyrazol-1-yl]pyridine ($pz^{R2}py$) in dry tetrahydrofurane was added the corresponding salt AgA in a 2:1 molar ratio under nitrogen atmosphere. The reaction was carried out in the darkness.

The mixture was stirred for 24 hours and then filtered through Celite. The clear filtrate was removed *in vacuo* and the solid crystallised from dichloromethane/hexane leading to the precipitation of a colourless solid, which was filtered off, washed with hexane and dried *in vacuo*.

[Ag($pz^{R2}py)_2$][PF_6] (R = $C_6H_4OC_{16}H_{33}$) (**1**): (Found: C, 68.6; H, 8.6; N, 4.8. $C_{104}H_{158}N_6O_4AgPF_6$ requires C, 68.9; H, 8.9; N, 4.6%); ν_{max}(KBr)/cm^{-1}: ν(CH) = 2917-2850vs, (ν(C=N) + ν(C=C)) = 1613 m, ν_{as}(PF) = 842vs, γ(CH) = 786w, γ(FPF) = 558w; δ_H(200 MHz; CDC_{13}; TMS) 0.84 (12 H, t, $^3J_{H,H}$ 6.8, CH_3), 1.26–1.67 (104 H, m, CH_2), 1.82 (8 H, m, CH_2), 3.73 (4 H, t, $^3J_{H,H}$ 6.5, OCH_2), 3.97 (4 H, t, $^3J_{H,H}$ 6.5, OCH_2), 6.64 (2 H, d, $^3J_{3,4}$ 8.1, H3), 6.66 (2 H, s, H4(pz)), 6.90 (4 H, d, $^3J_{H,H}$ 8.8, H_m), 6.96 (4 H, d, $^3J_{H,H}$ 8.8, H_m), 7.26 (4 H, d, $^3J_{H,H}$ 8.8, H_o), 7.41 (2 H, m, H5), 7.58 (4 H, d, $^3J_{H,H}$ 8.8, H_o), 7.69(2 H, m, H4(py)), 8.47 (2 H, d, $^3J_{5,6}$ 5.8, H6).

[Ag($pz^{R2}py)$][PF_6] (R = $C_6H_4OC_{18}H_{37}$) (**2**): (Found: C, 69.8; H, 8.8; N, 4.3. $C_{112}H_{174}N_6O_4AgPF_6$ requires C, 70.0; H, 9.1; N, 4.4%); ν_{max}(KBr)/cm^{-1}: ν(CH) = 2915-2859vs, (ν(C=N) + ν(C=C)) = 1615 m, ν_{as}(PF) = 841vs, γ(CH) = 785 w, γ(FPF) = 556 w; δ_H(200 MHz; $CDC1_3$; TMS): 0.87 (12 H, t, $^3J_{H,H}$ 6.8, CH_3), 1.25–1.59 (120 H, m, CH_2), 1.82 (8 H, m, CH_2), 3.77 (4 H, t, $^3J_{H,H}$ 6.5, OCH_2), 4.00 (4 H, t, $^3J_{H,H}$ 6.5, OCH_2), 6.67 (2 H, s, H4(pz)), 6.70 (2 H, d, $^3J_{3,4}$ 8.1, H3), 6.94 (4 H, d, $^3J_{H,H}$ 8.3, H_m), 6.99 (4 H, d, $^3J_{H,H}$ 8.6, H_m), 7.26 (4 H, d,

$^3J_{H,H}$ 8.3, H_o), 7.39 (2 H, m, H5), 7.63 (4 H, d, $^3J_{H,H}$ 8.6, H_o), 7.70 (2 H, m, H4(py)), 8.46 (2 H, d, $^3J_{5,6}$ 5.4, H6).

$[Ag(pz^{R2}py)_2][SbF_6]$ (R = $C_6H_4OC_{16}H_{33}$) (**3**): (Found: C, 65.7; H, 8.3; N, 4.4. $C_{104}H_{158}N_6O_4AgSbF_6$ requires C, 65.5; H, 8.1; N, 4.5%); ν_{max}(KBr)/cm^{-1}: ν(CH) = 2918-2851 vs, (ν(C=N) + ν(C=C)) = 1613 m, γ(CH) = 786 w, ν_{as}(SbF) = 660 s; δ_H(200 MHz; $CDCl_3$; TMS): 0.88 (12 H, t, $^3J_{H,H}$ 6.5, CH_3), 1.26–1.67 (104 H, m, CH_2), 1.82 (8 H, m, CH_2), 3.73 (4 H, t, $^3J_{H,H}$ 6.4, OCH_2), 4.00 (4 H, t, $^3J_{H,H}$ 6.4, OCH_2), 6.65 (2 H, d, $^3J_{3,4}$ 8.8, H3), 6.67 (2 H, s, H4(pz)), 6.91 (4 H, d, $^3J_{H,H}$ 8.5, H_m), 6.96 (4 H, d, $^3J_{H,H}$ 8.5, H_m), 7.26 (4 H, m, H_o), 7.39 (2 H, m, H5), 7.59 (4 H, d, $^3J_{H,H}$ 8.5, H_o), 7.69 (2 H, m, H4(py)), 8.43 (2 H, d, $^3J_{5,6}$ 4.4, H6).

$[Ag(pz^{R2}py)_2][SbF_6]$ (R = $C_6H_4OC_{18}H_{37}$) (**4**): (Found: C, 67.1; H, 8.6; N, 4.2. $C_{112}H_{174}N_6O_4AgSbF_6$ requires C, 66.8; H, 8.7; N, 4.1%); ν_{max}(KBr)/cm^{-1}: ν(CH) = 2916-2849vs, (ν(C=N) + ν(C=C)) = 1613 m, γ(CH) = 785 w, ν_{as}(SbF) = 659 s; δ_H(200 MHz; $CDCl_3$; TMS): 0.88 (12 H, t, $^3J_{H,H}$ 6.8, CH_3), 1.26–1.61 (120 H, m, CH_2), 1.82 (8 H, m, CH_2), 3.75 (4 H, t, $^3J_{H,H}$ 6.2, OCH_2), 4.00 (4 H, t, $^3J_{H,H}$ 6.2, OCH_2), 6.69 (2 H, d, $^3J_{3,4}$ 8.1, H3), 6.70 (2 H, s, H4(pz)), 6.96 (8 H, d, $^3J_{H,H}$ 8.3, H_m), 7.26 (4 H, m, H_o), 7.38 (2 H, m, H5), 7.61 (4 H, d, $^3J_{H,H}$ 8.2, H_o), 7.70 (2 H, m, H4(py)), 8.44 (2 H, d, $^3J_{5,6}$ 4.0, H6).

$[Ag(pz^{R2}py)_2][CF_3SO_3]$ (R = $C_6H_4OC_{16}H_{33}$) (**5**): (Found: C, 69.2; H, 8.5; N, 4.7. $C_{104}H_{158}N_6O_4AgCF_3SO_3$ requires C, 69.5; H, 8.8; N, 4.6%); ν_{max}(KBr)/cm^{-1}: ν(CH) = 2917-2851vs, (ν(C=N) + ν(C=C)) = 1613 m, $\nu_{as}(SO_3)$ = 1274, $\nu_s(SO_3)$ = 1029 m, γ(CH) = 786 w; δ_H(200 MHz; $CDCl_3$; TMS): 0.88 (12 H, t, $^3J_{H,H}$ 6.5, CH_3), 1.26–1.69 (104 H, m, CH_2), 1.83 (8 H, m, CH_2), 3.77 (4 H, t, $^3J_{H,H}$ 6.0, OCH_2), 4.00 (4 H, t, $^3J_{H,H}$ 6.4 OCH_2), 6.66 (2 H, s, H4(pz)), 6.69 (2 H, d, $^3J_{3,4}$ 8.0, H3), 6.92 (4 H, d, $^3J_{H,H}$ 7.7, H_m), 6.94 (4 H, d, $^3J_{H,H}$ 8.9, H_m), 7.26 (4 H, m, H_o), 7.40 (2 H, m, H5), 7.63 (4 H, d, $^3J_{H,H}$ 8.9, H_o), 7.72 (2 H, m, H4(py)), 8.57 (2 H, d, $^3J_{5,6}$ 5.0, H6).

$[Ag(pz^{R2}py)_2][CF_3SO_3]$ (R = $C_6H_4OC_{18}H_{37}$) (**6**): (Found: C, 70.7; H, 8.8; N, 4.7. $C_{112}H_{174}N_6O_4AgCF_3SO_3$ requires C, 70.5; H, 9.1; N, 4.4%); $\nu_{máx}$(KBr)/cm^{-1}: ν(CH) = 2917-2851vs, (ν(C=N) + ν(C=C)) = 1614 m, $\nu_{as}(SO_3)$ = 1278, $\nu_s(SO_3)$ = 1028 m, γ(CH) = 78l w; δ_H(200 MHz; $CDCl_3$; TMS): 0.88 (12 H, t, $^3J_{H,H}$ 6.3, CH_3), 1.26–1.69 (120 H, m, CH_2), 1.84 (8 H, m, CH_2), 3.87 (4 H, t, $^3J_{H,H}$ 6.0, OCH_2), 3.99 (4 H, t, $^3J_{H,H}$ 6.3 OCH_2), 6.70 (2 H, s, H4(pz)), 6.90 (4 H, d, $^3J_{H,H}$ 8.4, H_m), 6.92 (4 H, d, $^3J_{H,H}$ 8.1, H_m), 7.10 (2 H, d, $^3J_{3,4}$ 8.2, H3), 7.26 (4 H, m, H_o), 7.32 (2 H, m, H5), 7.82 (4 H, d, $^3J_{H,H}$ 8.4, H_o), 7.67 (2 H, m, H4(py)), 8.56 (2 H, d, $^3J_{5,6}$ 4.2, H6).

$[Ag(pz^{R2}py)_2][NO_3]$ (R = $C_6H_4OC_{16}H_{33}$) (**7**): (Found: C, 72.1; H, 9.5; N, 5.5. $C_{104}H_{158}N_6O_4AgNO_3$ requires C, 72.4; H, 9.2; N, 5.7%);

$\nu_{máx}$(KBr)/cm^{-1}: ν(CH) = 2916-2849vs, (ν(C=N) + ν(C=C)) = 1613 m, ν_d(NO) = 1384 m, γ(ONO) = 828 w, γ(CH) = 787 w; δ_H(200 MHz; $CDCl_3$; TMS): 0.88 (12 H, t, $^3J_{H,H}$ 6.5, CH_3), 1.26–1.67 (104 H, m, CH_2), 1.80 (8 H, m, CH_2), 3.95 (4 H, t, $^3J_{H,H}$ 6.4, OCH_2), 3.98 (4 H, t, $^3J_{H,H}$ 6.2, OCH_2), 6.71 (2 H, s, H4(pz)), 6.69 (2 H, d, $^3J_{3,4}$ 8.0, H3), 6.92 (4 H, d, $^3J_{H,H}$ 8.7, H_m), 6.94 (4 H, d, $^3J_{H,H}$ 8.9, H_m), 7.26 (4 H, m, Ho), 7.40 (2 H, m, H5), 7.63 (4 H, d, $^3J_{H,H}$ 8.9, H_o), 7.72 (2 H, m, H4(py)), 8.57 (2 H, d, $^3J_{5,6}$ 5.0, H6).

[Ag($pz^{R2}py$)$_2$][NO_3] (R = $C_6H_4OC_{18}H_{37}$) (**8**): (Found: C, 73.5; H, 9.8; N, 5.6. $C_{112}H_{174}N_6O_4AgNO_3$ requires C, 73.2; H, 9.5; N, 5.3%); ν_{max}(KBr)/cm^{-1}: ν(CH) = 2920-2850vs, (ν(C=N) + ν(C=C)) = 1615 m, ν_d(NO) = 1385 m, γ(ONO) = 825 w, γ(CH) = 785 w; δ_H(200 MHz; $CDCl_3$; TMS): 0.88 (12 H, t, $^3J_{H,H}$ 6.3, CH_3), 1.26–1.63 (120 H, m, CH_2), 1.78 (8 H, m, CH_2), 3.96 (4 H, t, $^3J_{H,H}$ 6.0, OCH_2), 3.96 (4 H, t, $^3J_{H,H}$ 6.3, OCH_2), 6.68 (2 H, s, H4(pz)), 6.85 (4 H, d, $^3J_{H,H}$ 8.5, H_m), 6.90 (4 H, d, $^3J_{H,H}$ 8.5, H_m), 7.20 (2 H, d, $^3J_{3,4}$ 8.5, H3), 7.26 (4 H, m, H_o), 7.32 (2 H, m, H5), 7.71 (2 H, m, H4(py)), 7.81 (4 H, d, $^3J_{H,H}$ 8.5, H_o), 8.48 (2 H, d, $^3J_{5,6}$ 4.0, H6).

Preparation of the Complexes [Zn($pz^{R2}py$)$_2$][NO_3]$_2$ *(R = $C_6H_4OC_nH_{2n+1}$; n = 16 (9), 18 (10))*

To a solution of the $Zn(NO_3)_2{\cdot}6H_2O$ in 5 mL of ethanol was added the corresponding 2-[3,5-bis(4-alkyloxy)phenyl]pyrazol-1-yl]pyridine ($pz^{R2}py$) in dichloromethane in a 1:2 molar ratio. The mixture was stirred for 48 hours and then was removed *in vacuo* and the solid crystallised from dichloromethane/ethanol leading to the precipitation of a colourless solid, which was filtered off, washed with hexane and dried *in vacuo*.

[Zn($pz^{R2}py$)$_2$][NO_3]$_2$ (R = $C_6H_4OC_{16}H_{33}$) (**9**): (Found: C, 71.2; H, 9.3; N, 5.9. $C_{104}H_{158}N_6O_4ZnN_2O_6$ requires C, 71.5; H, 9.1; N, 6.4%); ν_{max}(KBr)/cm^{-1}: ν(CH) = 2917-2849vs, (ν(C=N) + ν(C=C)) = 1611 m, ν_d(NO) = 1385 m, γ(ONO) = 840 w, γ(CH) = 777 w; δ_H(200 MHz; $CDCl_3$; TMS): 0.88 (12 H, t, $^3J_{H,H}$ 6.5, CH_3), 1.26–1.69 (104 H, m, CH_2), 1.80 (8 H, m, CH_2), 3.96 (4 H, t, $^3J_{H,H}$ 6.6, OCH_2), 4.02 (4 H, t, $^3J_{H,H}$ 6.6, OCH_2), 6.76 (2 H, s, H4(pz)), 6.95 (4 H, d, $^3J_{H,H}$ 8.6, H_m), 6.98 (4 H, d, $^3J_{H,H}$ 8.6, H_m), 7.17 (2 H, d, $^3J_{3,4}$ 8.0, H3), 7.31 (4 H, d, $^3J_{H,H}$ 8.8 H_o), 7.31 (2 H, m, H5), 7.72 (2 H, m, H4(py)), 7.76 (4 H, d, $^3J_{H,H}$ 8.8, H_o), 8.56 (2 H, d, $^3J_{5,6}$ 4.5, H6).

[Zn($pz^{R2}py$)$_2$][NO_3]$_2$ (R = $C_6H_4OC_{18}H_{37}$) (**10**): (Found: C, 72.1; H, 9.6; N, 5.7. $C_{112}H_{174}N_6O_4ZnN_2O_6$ requires C, 72.4; H, 9.4; N, 6.0%); ν_{max} (KBr)/cm^{-1}: ν(CH) = 2916-2851vs, (ν(C=N) + ν(C=C)) = 1612 m, ν_d(NO) = 1384 m, γ(ONO) = 839 w, γ(CH) = 779 w; δ_H(200 MHz; $CDCl_3$; TMS): 0.86 (12 H, t, $^3J_{H,H}$ 6.6, CH_3), 1.26–1.60 (120 H, m, CH_2), 1.81

(8 H, m, CH_2), 4.01 (4 H, t, $^3J_{H,H}$ 6.2, OCH_2), 4.04 (4 H, t, $^3J_{H,H}$ 6.4, OCH_2), 6.79 (2 H, s, H4(pz)), 7.01 (4 H, d, $^3J_{H,H}$ 8.1, H_m), 7.03 (4 H, d, $^3J_{H,H}$ 8.3, H_m), 7.06 (2H, d, $^3J_{3,4}$ 8.0, H3), 7.37 (4 H, d, $^3J_{H,H}$ 8.8 H_o), 7.39 (2 H, m, H5), 7.76 (2 H, m, H4(py)), 7.81 (4 H, d, $^3J_{H,H}$ 8.3, H_o), 8.60 (2 H, d, $^3J_{5,6}$ 4.2, H6).

Preparation of the Complexes [$ZnCl_2(pz^{R2}py)$] *($R = C_6H_4OC_nH_{2n+1}$; $n = 16$ (**11**), 18 (**12**), $n = 1$ (**13**))*

To a solution of the anhydrous $ZnCl_2$ in dry tetrahydrofurane was added the corresponding 2-[3,5-bis(4-alkyloxy)phenyl]pyrazol-1-yl]pyridine ($pz^{R2}py$) in dry tetrahydrofurane in a 1:1 molar ratio under nitrogen atmosphere. The mixture was stirred for 48 hours and then was removed *in vacuo* and the solid crystallised from dichloromethane/ethanol leading to the precipitation of a colourless solid, which was filtered off, washed with hexane and dried *in vacuo*.

[$ZnCl_2(pz^{R2}py)_2$] (R = $C_6H_4OC_{16}H_{33}$) (**11**): (Found: C, 68.1; H, 8.4; N, 4.7. $C_{52}H_{79}N_3O_2ZnCl_2$ requires C, 68.3; H, 8.7; N, 4.6%); $\nu_{máx}$(KBr)/cm^{-1}: ν(CH) = 2855-2788vs, (ν(C=N) + ν(C=C)) = 1610 m, γ(CH) = 782 w; δ_H(200 MHz; $CDCl_3$; TMS): 0.87 (6 H, t, $^3J_{H,H}$ 6.5, CH_3), 1.26–1.59 (52 H, m, CH_2), 1.85 (4 H, m, CH_2), 4.00 (2 H, t, $^3J_{H,H}$ 6.6, OCH_2), 4.07 (2 H, t, $^3J_{H,H}$ 6.6 OCH_2), 6.80 (1 H, s, H4(pz)), 6.97 (2 H, d, $^3J_{H,H}$ 8.8, H_m), 6.97 (1 H, d, $^3J_{3,4}$ 8.0, H3), 7.05 (2 H, d, $^3J_{H,H}$ 8.8, H_m), 7.26 (1H, m, H5), 7.40 (2 H, d, $^3J_{H,H}$ 8.0, H_o), 7.77 (1 H, m, H4(py)), 8.00 (2 H, d, $^3J_{H,H}$ 8.8 H_o), 8.60 (1 H, d, $^3J_{5,6}$ 4.5, H6).

[$ZnCl_2(pz^{R2}py)2$] (R = $C_6H_4OC_{18}H_{37}$) (**12**): (Found: C, 69.1; H, 8.7; N, 4.1. $C_{56}H_{87}N_3O_2ZnCl_2$ requires C, 69.3; H, 9.0; N, 4.3%); $\nu_{máx}$(KBr)/cm^{-1}: ν(CH) = 2848-2791vs, (ν(C=N) + ν(C=C)) = 1618 m, γ(CH) = 783 w; δ_H(200 MHz; $CDCl_3$; TMS): 0.88 (6 H, t, $^3J_{H,H}$ 6.4, CH_3), 1.26 – 1.58 (60 H, m, CH_2), 1.85 (4 H, m, CH_2), 4.02 (2 H, t, $^3J_{H,H}$ 6.4, OCH_2), 4.05 (2 H, t, $^3J_{H,H}$ 6.4 OCH_2), 6.80 (1 H, s, H4(pz)), 6.97 (2 H, d, $^3J_{H,H}$ 8.6, H_m), 6.97 (1 H, d, $^3J_{3,4}$ 8.0, H3), 7.06 (2 H, d, $^3J_{H,H}$ 8.6, H_m), 7.26 (1H, m, H5), 7.40 (2 H, d, $^3J_{H,H}$ 8.4, H_o), 7.77 (1 H, m, H4(py)), 8.00 (2 H, d, $^3J_{H,H}$ 8.6 H_o), 8.61 (1 H, d, $^3J_{5,6}$ 4.6, H6).

[$ZnCl_2(pz^{R2}py)_2$] (R = $C_6H_4OCH_3$) (**13**): (Found: C, 53.2; H, 4.0; N, 8.4. $C_{22}H_{19}N_3O_2ZnCl_2$ requires C, 53.5; H, 3.9; N, 8.5%); $\nu_{máx}$(KBr)/cm^{-1}: ν(CH) = 2858-2789vs, (ν(C=N) + ν(C=C)) = 1618 m, γ(CH) = 783 w; δ_H(200 MHz; $CDCl_3$; TMS): 3.50 (6 H, s, CH_3), 6.81 (1 H, s, H4(pz)), 6.96 (2 H, d, $^3J_{H,H}$ 8.6, H_m), 6.98 (1 H, d, $^3J_{3,4}$ 8.0, H3), 7.07 (2 H, d, $^3J_{H,H}$ 8.6, H_m), 7.26 (1H, m, H5), 7.42 (2 H, d, $^3J_{H,H}$ 8.4, H_o), 7.77 (1 H, m, H4(py)), 8.02 (2 H, d, $^3J_{H,H}$ 8.6 H_o), 8.61 (1 H, d, $^3J_{5,6}$ 4.6, H6).

X-ray Structure Determination of 13

Colourless prismatic single crystals ($0.11 \times 0.13 \times 0.13\,mm^3$) were grown by diffusion of hexane into a dichloromethane solution of the compound. *Crystal data*: $C_{22}H_{19}Cl_2N_3O_2Zn$; M_r 493.67; T296(2) K; monoclinic, space group $P2_1/c$, $a = 8.427(1)$, $b = 14.899(2)$, $c = 17.110(2)$ Å, $\beta = 99.400(2)^\circ$, $V = 2119.4(3)$ Å^3, $Z = 4$, $D_c = 1.547\,g\,cm^{-3}$, $\mu = 1.435\,mm^{-1}$. Data collection was carried out at room temperature on a Bruker Smart CCD diffractometer, with graphite-monochromated Mo-K_α radiation ($\lambda = 0.71073$ Å), operating at 50 kV and 25 mA. The data were collected over a hemisphere of the reciprocal space by combination of three exposure sets. The cell parameters were determined and refined by least-squares fit of all reflections collected [θ range = 1.82–25.00°; index range = (−10, −17, −20) to (9, 17, 20)]. Each exposure of 20 s covered 0.3° in ω. The first 100 frames were recollected at the end of the data collection to monitor crystal decay. No appreciable decay in the intensities of standard reflections was observed. The structure was solved by direct methods and conventional Fourier techniques. The refinement was made by full-matrix least-squares on F^2 [37]. Anisotropic parameters were used in the last cycles of refinement for all non-hydrogen atoms. Hydrogen atoms were included in calculated positions and refined as riding on their respective carbon atom with the thermal parameters related to the bonded atom. The final R indices with $I > 2\sigma(I)$ was 0.040 for 1857 observed reflections, while wR_2 for all data (3722 independent reflections, $R_{int} = 0.0978$) was 0.073. The GOF (F^2) was 0.781, and the largest residual peak and hole in the final difference map were 0.315 and −0.315 e Å^{-3}, respectively. CCDC-655618 contains the supplementary crystallographic data for this article.

CONCLUDING REMARKS

The silver(I) an zinc(II) complexes based on mesomorphic or non-mesomorphic *N,N′*-bidentate 2-[3,5-bis(4-alkyloxyphenyl)pyrazol-1-yl]pyridine ligands ($pz^{R2}py$) were prepared and the mesomorphic properties, investigated.

Complexes $[M(pz^{R2}py)_2][A]_m$ (M = Ag, m = 1; M = Zn, m = 2; **1–10**) showed to be metallomesogens exhibiting enantiotropic SmA mesophases in all cases, independently of the different coordination geometry around the metal. It appears that the 'H'-like molecular shape achieved through the planar MNNCN metallocycles involving the four elongated chains in an almost parallel fashion was determinant to produce lamellar mesophases.

For the neutral compounds $[ZnCl_2(pz^{R2}py)]$ (**11–12**), the rod-like features prevail over the achievement of smectic phases.

All SmA mesophases were characterized by POM and XRD studies. On cooling, the texture is maintained until 30°C; but not the mobility. At this temperature the XRD diffractograms suggest a lamello-columnar (ColL) mesophase within the ordered smectic-layers.

REFERENCES

[1] Mayoral, M. J., Torralba, M. C., Cano, M., Campo, J. A., & Heras, J. V. (2003). *Inorg. Chem. Commun.*, *6*, 626.
[2] Torralba, M. C., Campo, J. A., Heras, J. V., Bruce, D. W., & Cano, M. (2006). *Dalton Trans.*, 3918.
[3] Pucci, D., Barberio, G., Bellusci, A., Crispini, A., Ghedini, M., & Ildyko Szerb, E. (2005). *Mol. Cryst. Liq. Cryst.*, *441*, 251.
[4] Constable, E. C., Housecroft, C. E., Neuburger, M., Poleschak, I., & Zehnder, M. (2003). *Polyhedron*, *22*, 93.
[5] Wu, H.-P., Janiak, C., Rheinwald, G., & Lang, H. (1999). *J. Chem. Soc, Dalton Trans.*, 183.
[6] Gallego, M. L., Cano, M., Campo, J. A., Heras, J. V., Pinilla, E., Torres, M. R., Cornago, P., & Claramunt, R. M. (2005). *Eur. J. Inorg. Chem.*, 4370.
[7] See for example: Serrano, J. L. ed. (1996). *Metallomesogens: Synthesis, Properties and Applications*. VCH: Weinheim.
[8] Lee, C.-K., Ling, M.-J., & Lin, I. J. B. (2003). *Dalton Trans.*, 4731.
[9] Giménez, R., Manrique, A. B., Uriel, S., Barbera, J., & Serrano, J. L. (2004). *Chem. Commun.*, 2064.
[10] Torralba, M. C., Cano, M., Campo, J. A., Heras, J. V., Pinilla, E., & Torres. M. R. (2006). *J. Organomet. Chem.*, *691*, 765.
[11] Torralba, M. C., Cano, M., Campo, J. A., Heras, J. V., Pinilla, E., Torres, M. R., Perles, J., & Ruiz-Valero, C. (2006). *J. Organomet. Chem.*, *691*, 2614.
[12] Nakamoto, K. (1986). *Infrared and Raman Spectra of Inorganic and Coordination Compounds*, 4th Ed. Wiley: New York.
[13] Awaleh, M. O., Badia, A., & Brisse, F. (2005). *Inorg. Chem.*, *44*, 7833.
[14] Lawrance, G. A. (1986). *Coord. Chem. Rev.*, *86*, 17.
[15] Zhong, J. C., Munakata, M., Kuroda-Sowa, T., Maekawa, M., Suenaga, Y., & Konaka, H. (2001). *Inorg, Chem.*, *40*, 3191.
[16] Gallego, M. L., Cano, M., Campo, J. A., Heras, J. V., Pinilla, E., & Torres, M. R. (2005). *Helv. Chim. Acta*, *88*, 2433.
[17] Matsumoto, K., Hagiwara, R., Ito, Y., & Tamada, O. (2002). *Solid State Sci.*, *4*, 1465.
[18] Reger, D. L., Semeniuc, R. F., Rassolov, V., & Smith, M. D. (2004). *Inorg. Chem.*, *43*, 537.
[19] Jung, O. S., Kim, Y. J., Lee, Y. A., Chae, H. K., Jang, H. G., & Hong, J. (2001). *Inorg. Chem.*, *40*, 2105.
[20] Chen, Y. D., Zhang, L. Y., Shi, L. X., & Chen, Z. N. (2004). *Inorg. Chem.*, *43*, 7493.
[21] Ghosh, P., Wood, M., Bonnano, J. B., Hascall, T., & Parkin, G. (1999). *Polyhedron*, *18*, 1107.
[22] Balamurugan, V., Hundal, M. S., & Mukherjee, R. (2004). *Chem. Eur. J.*, *10*, 1683.
[23] Bouwman, E., Driessen, W. L., de Graaf, R. A. G., & Reedijk, J. (1984). *Acta Crystallogr, Sect.C: Cryst. Strud. Commun.*, *40*, 1562.

[24] Bovio, B., Cingolani, A., & Bonati, F. (1992). *Z. Anorg. Allg. Chem.*, *610*, 151.
[25] Bieller, S., Haghiti, A., Bolte, M., Bats, J. W., Wagner, M., & Lerner, H.-W. (2006). *Inorg. Chim. Acta*, *359*, 1559.
[26] Cheng, M.-L., Li, H.-X., Yong, Z., & Lang, J.-P. (2006). *Acta Crystallogr. Sect.C: Cryst. Strud. Commun.*, *62*, m74.
[27] Crew, M. G. B., Tocher, D. A., Chowdhury, K., Chowdhury, S., & Datta, D. (2004). *New. J. Chem.*, *28*, 323.
[28] Abe, Y., Akao, H., Yoshida, Y., Takashima, H., Tanase, T., Mukai, H., & Ohta, K. (2006). *Inorg. Chim. Acta*, *359*, 3147.
[29] Ohta, K., Muroki, H., Takagi, A., Hatada, K., Ema, H., Yamamoto, I., & Matsuzaki, K. (1986). *Mol. Cryst. Liq. Cryst.*, *140*, 131.
[30] El-ghayoury, A., Douce, L., Skoulius, A., & Ziessel, R. (1998). *Angew. Chem. Int. Ed.*, *37*, 1255.
[31] Mery, S., Haristoy, D., Nicoud, J.-F., Guillon, D., Diele, S., Monobe, H., & Shimizu, Y. (2002). *J. Mater. Chem.*, *12*, 37.
[32] Cardinaels, T., Driesen, K., Parac-Vogt, T. N., Heinrich, B., Bourgogne, C., Guillon, D., Donnio, B., & Binnemans, K. (2005). *Chem. Mater*, *17*, 6589.
[33] Barberá, J., Donnio, B., Gehringer, L., Guillon, D., Marcos, M., Omenat, A., Serrano. J. L. (2005). *J. Mater. Chem.*, *15*, 4093.
[34] Terazzi, E., Torelli, S., Bernardinelli, G., Rivera, J. P., Vence, J. M., Bourgogne, C., Donnio, B., Guillon, D., Imbert, D., Bunzli, J. C. G., Pinto, A., Jeannerat, D., & Piguet, C. (2005). *J. Am. Chem. Soc*, *127*, 888.
[35] Chien, C. W., Liu, K. T., & Lai, C. K. (2004). *Liq. Cryst.*, *31*, 1007.
[36] Tschierske, C. (1998). *J. Mater. Chem.*, *8*, 1485.
[37] Sheldrick, G. M. (1997). *SHELXL97, Program for Refinement of Crystal Structure*, University of Göttingen: Göttingen, Germany.